Heat Transfer Between Fluidized-solids Beds and Boundary Surfaces—Correlation of Data

LEONARD WENDER and GEORGE T. COOPER

The M. W. Kellogg Company, New York, New York

A broad empirical study of nine independent sets of data on fluidized-bed heat transfer is presented, with correlation of the data in two groups. A wide range of the many variables is covered, and some data on commercial units are included. Data for external (i.e., walls of the fluidizing vessel) and internal (i.e., tubes in the bed) heat transfer surfaces are correlated graphically. The correlations indicate the importance of heat transport by the mobile particles and of unsteady state conduction in the gas.

The problem of determining heat transfer coefficients between beds of fluidized solids and boundary surfaces (either the walls of the fluidizing vessel or tubes immersed in the bed) has attracted the attention of numerous investigators in recent years. Papers presenting data on such coefficients have been those of Bartholomew and Katz (*3*), Dow and Jakob (*7*), Mickley and Trilling (*21*), Toomey and Johnstone (*26*), Baerg, Klassen, and Gishler (*2*), Leva, Weintraub, and Grummer (*16*), Leva (*15*), Olin and Dean (*23*), Mickley and Fairbanks (*20*), Van Heerden, Nobel, and Van Krevelen (*29, 30*), Pritzlaff (*24*), Brazelton (*4*), Levenspiel and Walton (*18, 19*), Simon (*25*), Miller and Logwinuk (*22*), Jolley (*11*), Campbell and Rumford (*5*), Agarwal and Storrow (*1*), and Vreedenberg (*31, 32*).

Review papers or papers presenting special limited data have been those of Gamson (*8*), Van Heerden, Nobel, and Van Krevelen (*27, 28*), Leva and Grummer (*14*), Wen and Leva (*35*), and Gilliland (*9*). Papers dealing with heat transfer between the solid particles and the gas stream are those of Kettenring, Manderfield, and Smith (*12*), Walton, Olson and Levenspiel (*33*), and Wamsley and Johanson (*34*). Koble, Ademino, Bartkus, and Corrigan (*13*) studied dense-phase transport, and dilute phase transport was investigated by Pritzlaff (*24*). Carr and Amundson (*6*) presented a mathematical study.

Unpublished data were also available to the authors on commercial fluid-hydroformer–catalyst regenerators built by The M. W. Kellogg Company.

Of all the papers listed above, only one was a general correlation attempt, using more than one set of data to establish a correlation. That was the paper of Wen and Leva. Of course, many of the authors listed presented correlations for their own data, but none of these limited correlations appeared to be able to encompass many other data. The lack of theoretical understanding of mechanism and of general correlation work has left the problem of predicting fluidized-bed heat transfer coefficients in a chaotic state. The situation was well summarized by Van Heerden (*28*), who reviewed the picture and for comparison tabulated some of the proposed correlation equations. Using these to predict coefficients for four hypothetical cases, he found the predicted values to cover an enormous range—248-fold for one of the cases. The correlations proposed here, while empirical, do indicate that order can be brought into the situation, and it is hoped that these results will encourage other workers in the field to continue so that the problem of fluidized-bed heat transfer may be fully understood.

METHOD OF ATTACK

Of the data listed above, not all were used in this work. Some were not used because of lack of reporting of variables found to be necessary, and others because of time limitations. Among those used, some were not fully worked up because of time limitations; however, the substantial numbers of runs which were fully worked up are representative of the data in those cases. Data which were completely worked up are those of Bartholomew and Katz, of Dow and Jakob, of Mickley and Trilling, of Toomey and Johnstone, and of Baerg, Klassen, and Gishler. [In the last case, pressure drops for fraction solids calculation were supplied (*10*) to the authors for most, but not all, runs.] Those largely but incompletely covered are the data of Leva, Weintraub, and Grummer, of Mickley and Fairbanks, and of Olin and Dean. (The extensive data of Van Heerden, Nobel, and Van Krevelen were not worked up because of lack of values of bed density or fraction solids.)

Owing to the general lack of quantitative understanding of mechanism, it was decided to use an empirical approach in which the data would be permitted to "tell their story" and which would involve a minimum of preconceived notions as to the variables involved. Dimensional analysis was thus rejected. A laborious procedure of successive cross plotting to evaluate the effect of each variable—as it was found to exert an effect—was chosen, to be used as the data allowed. The over-all result was something of a "brute force" attack on the problem, but this was felt to be necessary in order

first to establish whether the various data could be hammered into some sort of cohesion before any very elegant refinements were attempted.

Study was limited to heat transfer between a bed and heat transfer surfaces (as against transfer between the solid particles and the gas). Continuous vertical transport was not studied.

CORRELATION OF EXTERNAL HEAT TRANSFER SURFACE DATA

High L_H/D_T Data as Start, Effect of Fraction Solids

Preliminary consideration was limited to data on external heat transfer surface. By this is meant operation with heat transferred between the bed and the walls of the fluidizing vessel. (It was later found that transfer between the bed and internal tubes requires a separate correlation.)

Van Heerden, et al. (*27*, *28*) showed that a bed-height (L_B) effect reported by Dow and Jakob is in reality a heated-length (L_H) effect and one in which coefficients decrease and then level off to a constant value as L_H increases. Figure 1 shows Van Heerden's curve of h vs. L_H. It was evident that a good start would be had with data at a high and constant L_H/D_T, preferably above 5, the point at which Van Heerden's curve, converted to h vs. L_H/D_T, leveled off. In this manner a complex L_H/D_T effect would not be present to obscure the effect of other variables, and the wide L_H/D_T range data of Dow and Jakob could later be used to study this factor.

The data of Bartholomew and Katz suited this requirement well. This was a study of heat transfer from the walls of a 4-in. pipe to sand, calcium carbonate, and aluminum powder, respectively, fluidized with air. L_H/D_T was kept constant at 7.5 and the work covered a wide range of air velocity, particle size, and fraction solids.

An arbitrary decision was made (subject to change if found necessary) to start with h in the Nusselt number hD_p/k_g, or Nu_p and with mass velocity G in the Reynolds number D_pG/μ, or Re_p. (Some authors used G/G_{mf} instead of Re_p, but the latter was considered more convenient.) Curves of Nu_p vs. Re_p for sand-air data of Bartholomew and Katz, such as in Figure 2, showed separation according to average particle size D_p. They also showed maxima, due presumably to increased particle motion causing h to increase with G, with this factor being offset at high velocities by reduced solids concentration. The introduction of fraction solids, $1 - \epsilon$, seemed a profitable approach, and from Bartholomew and Katz data, as curves of $1 - \epsilon$ vs. Re_p at constant D_p, a cross plot was made, at constant Re_p, of Nu_p vs. $1 - \epsilon$ (Figure 3). (These data are for runs at 400°F. wall temperature. Their data at 600°F. wall

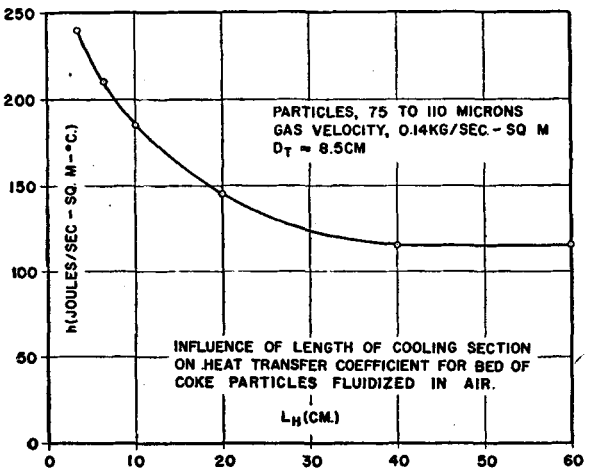

Fig. 1. Data of Van Heerden.

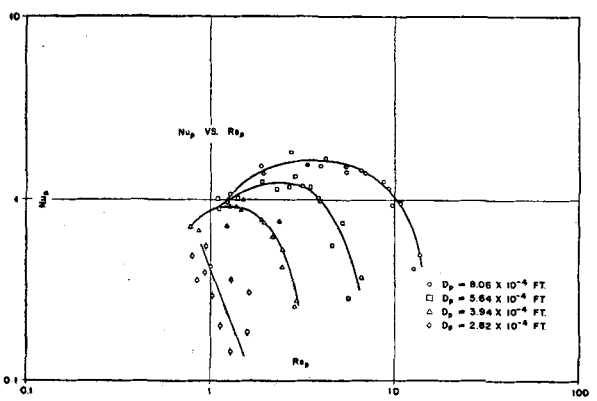

Fig. 2. Bartholomew and Katz sand-air data for narrow-size fractions; 400°F. wall temperature.

emperature are discussed below.) The points, which include both narrow and wide D_p ranges, lie on a straight line of slope 1.0, indicating proportionality of Nu_p to $1 - \epsilon$. A plot of $Nu_p/(1 - \epsilon)$ was then found to tie all these data of Figure 2 together on one smooth curve, with no maximum and no separation according to D_p (Figure 4). The group $Nu_p/(1 - \epsilon)$, plotted against Re_p, apparently takes care of the effects of D_p, G, and $1 - \epsilon$.

A composite plot of $Nu_p/(1 - \epsilon)$ vs. Re_p over an L_H/D_T range of 7 to 36, for the data of other authors as well as Bartholomew and Katz, showed a smooth curve with some spreading due to physical-properties variations for different systems, but no discernible effect of L_H/D_T. It was concluded that $L_H/D_T > 7$ was safe for physical-properties study, being in the region where L_H/D_T is high enough to be without effect.

Physical Properties, the Group $c_s\rho_p/c_g\rho_g$

Data of Bartholomew and Katz at 600°F. wall temperature were found to plot a bit high, relative to 400°F. wall temperature data, on a $Nu_p/(1 - \epsilon)$ vs. Re_p curve. The former data were at higher bed temperatures, causing some difference in gas properties. Vreedenberg (*31*) had suggested use of the ratio of gas density to particle density ρ_g/ρ_p as a multiplier on the coefficient, and it was found that this factor promoted an excellent line-up of the high- and low-temperature data of Bartholomew and Katz.

Attention was then turned to the data of Leva, Weintraub, and Grummer (*16*), who covered a wide range of physical properties. [Their reported coefficients were based on area corresponding to bed height at incipient fluidization L_{mf}, and ΔT values were determined by using values of bed temperature T_B integrated over the length L_{mf}. Their data were recalculated to obtain coefficients based on heated length L_H. In addition, their reported gas-inlet temperatures were in error, and their data were therefore recalculated to a basis of 80°F. gas-inlet temperature, which was believed to have been approximately correct (*17*).] Their runs at $L_H/D_T > 7$ were plotted as $Nu_p/(1 - \epsilon)$ and $Nu_p/[(1 - \epsilon)(\rho_p/\rho_g)]$ vs. Re_p, the latter showing a distinct advantage. However, their helium data (high gas-heat capacity c_g) deviated, indicating the need for inclusion of heat capacity, it being noted that use of a gas-to-solid heat-capacity ratio c_g/c_s as a direct multiplier on Nu_p would bring these data into line with the others.

The combined-properties group $c_s\rho_p/c_g\rho_g$ was used by Dow and Jakob and by Van Heerden, Nobel, and Van Krevelen, and its use here as $Nu_p/[(1 - \epsilon)(c_s\rho_p/c_g\rho_g)]$ was indicated. A cross plot of $Nu_p/(1 - \epsilon)$ vs. $c_s\rho_p/c_g\rho_g$, at constant Re_p, was prepared (Figure 5) from curves of $Nu_p(1 - \epsilon)$ vs. Re_p for

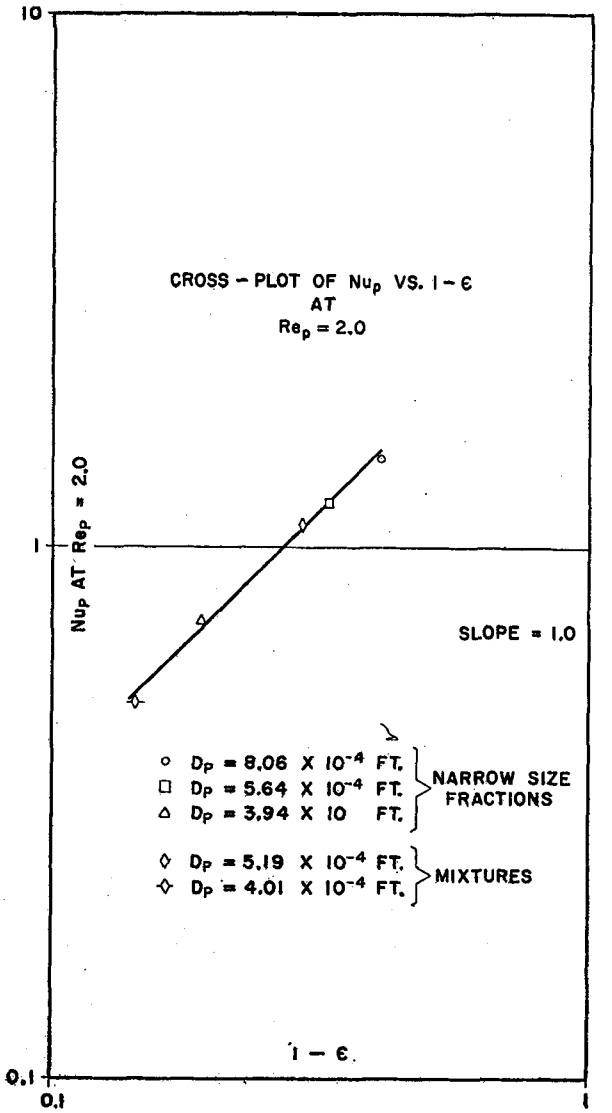

Fig. 3. Bartholomew and Katz sand-air data; 400°F. wall temperature.

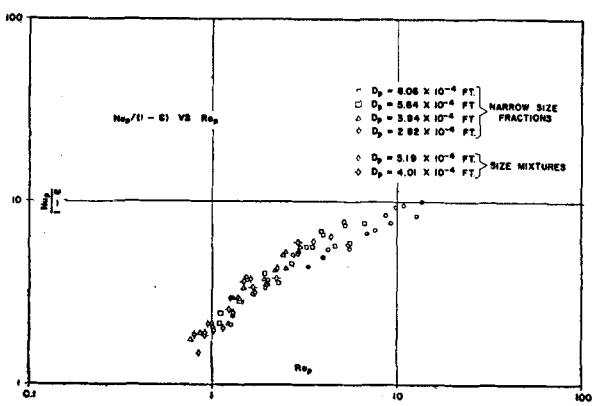

Fig. 4. Bartholomew and Katz sand-air data; 400°F. wall temperature.

constant system properties, using data at $L_H/D_T > 7$ of Leva, et al., and others. (See Table 1.) The points can be represented adequately by a line of slope 1.0, an indication of the applicability of $Nu_p/(1 - \epsilon)$ proportional to $c_s\rho_p/c_g\rho_g$. (Note: the subscript p was used in ρ_p to define this term specifically as particle density, including intraparticle voids when present, whereas c_s represents heat capacity of the solid.)

It was concluded that a correlation could be obtained by plotting $Nu_p/[(1 - \epsilon)(c_s\rho_p/c_g\rho_g)]$ vs. Re_p. For convenience, the correlation group $Nu_p/[(1 - \epsilon)(c_s\rho_p/c_g\rho_g)]$ is designated as y. Figure 6 shows y vs. Re_p for data at $L_H/D_T > 7$ from the four sources worked up.

Quantitative Treatment of L_H/D_T Effect

Extension to $L_H/D_T < 7$

Some of the data of Leva, Weintraub, and Grummer and of Toomey and Johnstone, and all the data of Dow and Jakob are at L_H/D_T less than 7. The Dow and Jakob data cover a wide range of L_H/D_T and are useful for evaluating its place in the correlation.

The Van Heerden curve, with h decreasing with L_H and then leveling off to a constant value, suggested use of a "dying-away" or "decaying" function of the form $h = h_0 + h_0Be^{-CL_H}$, where h_0 is the constant value reached by h at high L_H, rather than the simple 0.65 power function used by Dow and Jakob. As a test, the data of Van Heerden's L_H study shown in Figure 1 were redrawn as a semilog plot of $h/h_0 - 1$ vs. L_H, with $h_0 = 115$ joules/(sec.)(sq. meter/ °C.). A straight line was obtained, which confirmed applicability of this function.

Application was then made to the Dow and Jakob data as follows. Over the Re_p range involved, the Dow and Jakob data show $Nu_p/(1 - \epsilon)$ proportional to $(Re_p)^{0.8}$, as reported by them. These data were worked up as $y/(Re_p)^{0.8}$, this combined function representing their data transposed to a Re_p of 1 for study of L_H effect. E designates y at $Re_p = 1$; and for Dow and Jakob, $E = y/(Re_p)^{0.8}$. (Cross plotting from lines of constant L_H/D_T could also have been used.) Comparison of plots of E vs. L_H and E vs. L_H/D_T for their coke data, obtained in 2- and 3-in. units, confirmed need for L_H as L_H/D_T. Separation of their Aerocat cracking catalyst, coke, and iron-powder data (all fluidized with air) when plotted as E vs. L_H/D_T indicated need for some additional properties term with L_H/D_T. Cross plots were made of L_H/D_T, at constant E, vs. ρ_p/ρ_g, c_s/c_g, and $c_s\rho_p/c_g\rho_g$. On the basis (admittedly sketchy) of obtaining a straight line of slope 1.1 on the c_s/c_g plot, it was decided to use the L_H/D_T group as $(L_H/D_T)/(c_s/c_g)$, here designated ϕ. (Van Heerden explains the variation of h with L_H as due

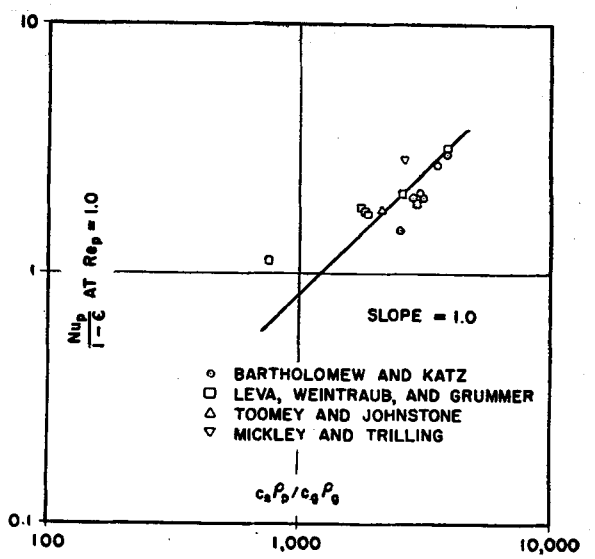

Fig. 5. Physical-properties cross plot for external surface; from data at $L_H/D_T > 7$.

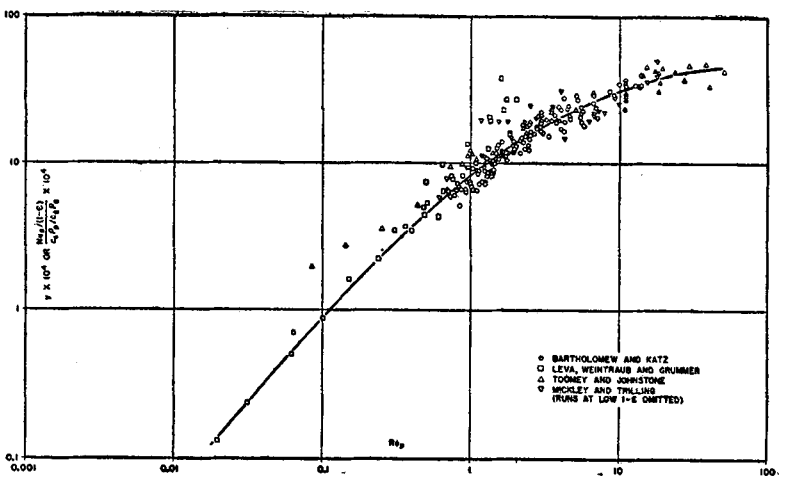

Fig. 6. Plot of y vs. Re_p for external heat transfer surface at $L_H/D_T > 7$.

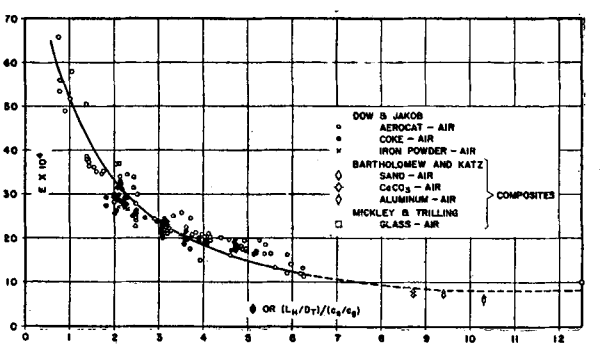

Fig. 7. E vs. ϕ for external surface.

to gradual establishment of a stationary temperature gradient in the downward-moving surface layer commonly observed at the wall of a fluidized bed. If so, then thermal properties may very well be involved.) Figure 7 shows E vs. ϕ for the Dow and Jakob data (individual runs) and for other data (composite values from cross plotting). (Data of Leva, Weintraub, and Grummer inexplicably show no L_H effect and are omitted in Figure 7.) It can be seen that Dow and Jakob data on Aerocat, coke, and iron powder fall together and that they extrapolate reasonably well to the high ϕ data of other workers. This tie-in of several authors' results was most encouraging.

A semilog plot of $E/E_0 - 1$ vs. ϕ was used for evaluation of constants B and C in the decaying function $y = y_0(1 + Be^{-C\phi})$. Rearranging and writing for use of E gives $E/E_0 - 1 = Be^{-C\phi}$. (The subscript 0 refers to the region of high L_H/D_T, where h is constant.) Selection of a proper value of E_0 was necessary in order to prepare this graph. Since Figure 6 represents data in the region where the L_H effect has essentially vanished, the value of y_0 at $Re_p = 1$ can be estimated from this graph. Inspection of Figure 6 yields 8.0×10^{-4} as a suitable value of y_0 at $Re_p = 1$, or E_0. In Figure 7 the Dow and Jakob data are shown satisfactorily extrapolated to this value of E_0. From the semilog plot of $E/E_0 - 1$ vs. ϕ, B and C were obtained as 7.5 and 0.44 respectively. The L_H-group correction factor becomes $1 + 7.5e^{-0.44\phi}$. Calling this F makes the final correlation group, then,

$$\frac{hD_p/[k_g(1-\epsilon)(c_s\rho_p/c_g\rho_g)]}{1+7.5e^{-0.44(L_H/D_T)/(c_s/c_g)}} \quad \text{or} \quad \frac{y}{F}$$

Figure 8, y/F vs. Re_p, shows the data of Dow and Jakob; of Bartholomew and Katz; of Leva, Weintraub, and Grummer; of Mickley and Trilling; and of Toomey and Johnstone (approximate bed heights estimated from inspection of individual section pressure drops for their sectionalized apparatus and may include dilute phase above dense bed) and is presented as a correlation for the case of external heat transfer surface. The average deviation is 22.1% for the 429 points. The low ϕ data of Leva et al. deviate the most seriously of the points plotted. Major deviations of the low-bed-density runs of Mickley and Trilling are not shown, but are discussed later.

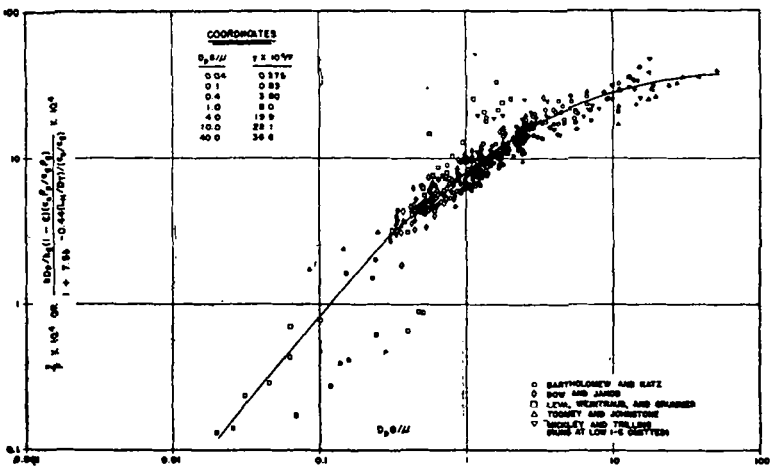

Fig. 8. The y correlation for external heat transfer surface.

CORRELATION OF INTERNAL HEAT TRANSFER SURFACE DATA

Physical Properties

Data which have been worked up for the case of internal heat transfer surface are those of Mickley and Fairbanks; Olin and Dean; Baerg, Klassen, and Gishler; Toomey and Johnstone; Mickley and Trilling; and Kellogg-built commercial fluid-hydroformer-catalyst-regenerator bed coolers. These data did not check out with the y correlation, and need for a separate correlation was apparent.

Owing to lack of suitable data covering a wide range of fraction solids, proportionality of Nu_p to $1 - \epsilon$ was assumed on the basis of its having been established for the external surface case. (Some confirmatory evidence has since become available on the commercial units.) No L/D effect was observed for the internal surface data although L_B/D_T ranged ninefold and L_H/D_T fifteenfold.

Physical-properties effects were evaluated from the excellent data of Mickley and Fairbanks, who covered a wide range of gas properties. Their data when plotted as $Nu_p/(1-\epsilon)$ vs. Re_p showed a family of lines for the different systems used. (See Table 2 for a summary of physical-properties terms.) Cross plotting of $Nu_p/(1-\epsilon)$, at constant Re_p vs. $c_s\rho_p/c_g\rho_g$ yielded no correlation; however, trial-and-error log-paper plotting of $Nu_p/[(1-\epsilon)(c_s/c_g)^n]$ vs. ρ_p/ρ_g with various values of n yielded a good line-up of points when $n = 0.80$, the slope of the line being 0.66. This indicated suitability of $Nu_p/[(1-\epsilon)(c_s c_g)^{0.80}(\rho_p/\rho_g)^{0.66}]$. However, the helium and dichlorodifluoromethane (Freon 12) points did not line up with the others, an indication of a need for some additional group which has essentially the same value for all the other gases but which has markedly different values for helium and dichlorodifluoromethane. Inspection of properties (Table 2) showed

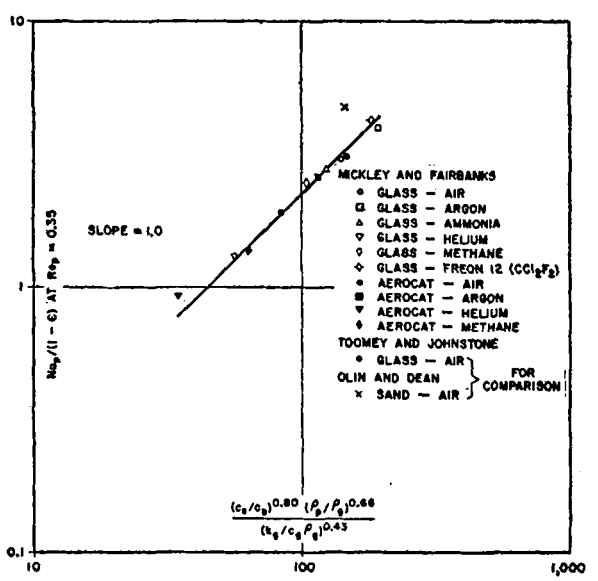

Fig. 9. Physical-properties cross plot for internal surface.

thermal diffusivity $k_g/c_g\rho_g$ to fit this requirement. A log plot of $Nu_p/[(1-\epsilon)(c_s/c_g)^{0.80}(\rho_p/\rho_g)^{0.66}]$ vs. $k_g/c_g\rho_g$ caused helium and dichlorodifluoromethane data to line up with the others on a slope of -0.43. (Kinematic viscosity μ/ρ_g behaves essentially the same, since values of Prandtl number vary little.) Figure 9 shows $Nu_p/(1-\epsilon)$ plotted against the combined-properties group $(c_s/c_g)^{0.80}(\rho_p/\rho_g)^{0.66}/(k_g/c_g\rho_g)^{0.43}$. Accordingly, the final-correlation group becomes

$$\frac{\dfrac{hD_p}{k_g(1-\epsilon)}\left(\dfrac{k_g}{c_g\rho_g}\right)^{0.43}}{\left(\dfrac{c_s}{c_g}\right)^{0.80}\left(\dfrac{\rho_p}{\rho_g}\right)^{0.66}} \quad \text{or} \quad z$$

This is not dimensionless, $k_g/c_g\rho_g$ having net units of square feet per hour. For convenience, the entire group is labeled z.

When plotted against Re_p, the z group showed tight correlation of the data of Mickley and Fairbanks (Figure 10) and a general correlation of these data with those of Olin and Dean; Toomey and Johnstone; Baerg, Klassen, and Gishler; and Mickley and Trilling. However, these data are all for axial tube location, and data of Kellogg-built commercial fluid-hydroformer–catalyst regenerators having multiple cooling tubes located between shell axis and shell wall plotted somewhat high.

Correction for Nonaxial-tube Location

It was recalled that Vreedenberg (*31*) studied the effect of tube location, using a vertical tube at three locations (including axial) at constant operating conditions. His results are shown in Figure 11 as h/h_{axial} vs. R_t/R_T, the ratio of radial-tube distance from the center line to the radius of the shell. The effect of tube location is substantial. The ratio h/h_{axial} was designated as a correction factor C_R for nonaxial tube location and the z correlation was modified to z/C_R vs. Re_p. (Of course, for all axial-tube data $C_R = 1$.) Figure 12 shows the final correlation and includes the data mentioned above plus six points calculated from operating data on three commercial fluid-hydroformer–catalyst–regenerator bed coolers which, with use of the C_R factor, now fall in with the axial-tube data. These commercial units represent a substantial scale-up relative to the laboratory units used by those workers from whose data the z correlation was developed.

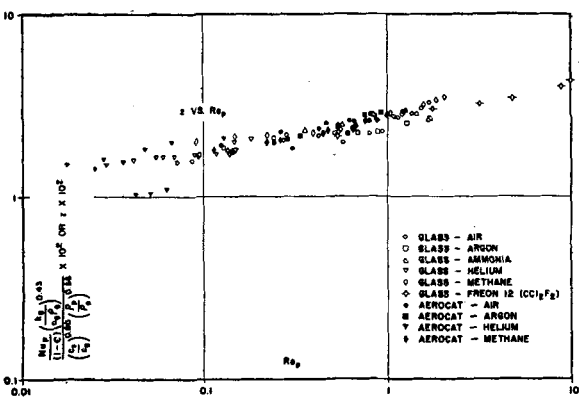

Fig. 10. Data of Mickley and Fairbanks.

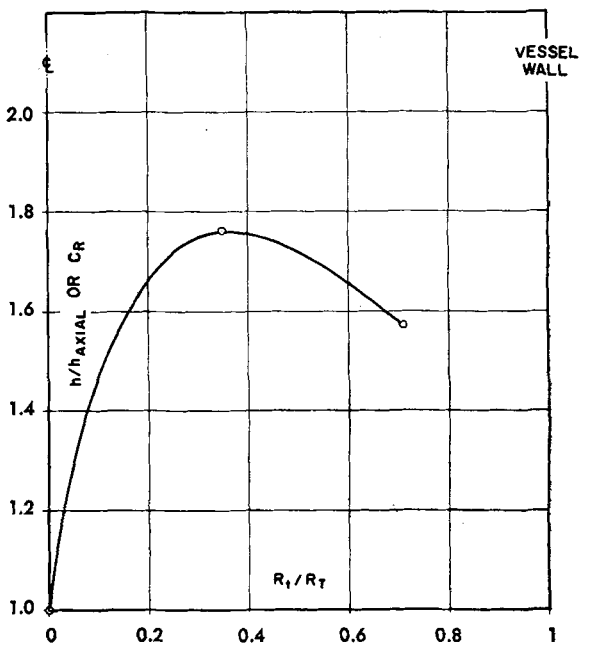

Fig. 11. Data of Vreedenberg for correction for nonaxial tube location in case of internal (inserted) surface.

TABLE 1

TERMS FOR EXTERNAL HEAT-TRANSFER SURFACE,

$L_H/D_T > 7.0$

$Nu_p/(1-\epsilon)$ at $Re_p = 1.0$ as a Function of Physical Properties

Source	Solid	Gas	Identification	ρ_p	ρ_g	c_s	c_g	$c_s\rho_p/c_g\rho_g$	k_g	$k_g/c_g\rho_g$, sq. ft./hr.	$\frac{Nu_p}{1-\epsilon}$ at $Re_p = 1.0$	$\frac{hD_p}{(1-\epsilon)c_s\rho_p}$ at $Re_p = 1.0$
3	Sand	Air	600°F. Wall	165	0.038	0.20	0.25	3,500	0.0268	2.83	2.72	0.00221
3	Sand	Air	400°F. Wall	165	0.047	0.20	0.25	2,800	0.0225	1.91	2.02	0.00138
3	$CaCO_3$	Air	600°F. Wall	167	0.038	0.214	0.25	3,800	0.0268	2.83	3.00	0.00225
3	$CaCO_3$	Air	400°F. Wall	167	0.047	0.214	0.25	3,000	0.0225	1.91	2.10	0.00132
3	Aluminum	Air	600°F. Wall	160	0.038	0.182	0.25	3,100	0.0268	2.83	2.01	0.00185
3	Aluminum	Air	400°F. Wall	160	0.047	0.182	0.25	2,500	0.0225	1.91	1.50	0.00116
21	Glass	Air	$c_s\rho_p/c_g\rho_g$ = 2,600	153	0.047	0.20	0.25	2,600	0.0234	1.99	2.85	0.00218
26	Glass	Air		175	0.067	0.20	0.25	2,100	0.0180	1.07	1.80	0.000928
16	Sand	Air	Run 28	165	0.0734	0.20	0.25	1,800	0.0216	1.18	1.72	0.00113
16	Sand	Air	Run 57	165	0.0514	0.20	0.25	2,570	0.0216	1.68	2.10	0.00138
16	Sand	CO_2	Run 5	165	0.1845	0.20	0.235	764	0.0170	0.392	1.12	0.000576
16	Sand	CO_2	Run 4	165	0.0775	0.20	0.235	1,810	0.0170	0.935	1.72	0.00109
16	Sand	Helium	Run 56	165	0.0069	0.20	1.24	3,860	0.108	12.6	3.2*	0.0104*
16	Iron catalyst	Air	Run 39	312	0.135	0.193	0.25	1,770	0.0216	0.641	1.80	0.000645
16	Iron catalyst	Air	Run 46	312	0.0818	0.193	0.25	2,920	0.0216	1.05	1.91	0.000685

*Extrapolated value. Curve of $Nu_p/(1-\epsilon)$ vs. Re_p extrapolated to have same slope at $Re_p = 1$ as the other curves of Leva, et. al.

The equation of the straight line of Figure 12 is

$$\left(\frac{hD_p/k_g}{1-\epsilon}\right)\left(\frac{k_g}{c_g\rho_g}\right)^{0.43} = 0.033C_R\left(\frac{D_pG}{\mu}\right)^{0.23}\left(\frac{c_s}{c_g}\right)^{0.80}\left(\frac{\rho_p}{\rho_g}\right)^{0.66}$$

with C_R being read from Figure 11. The group $k_g/c_g\rho_g$ has net units of square feet per hour. This is presented as the correlation for internal heat transfer surface. Average deviation for the 323 points plotted is 19.5%.

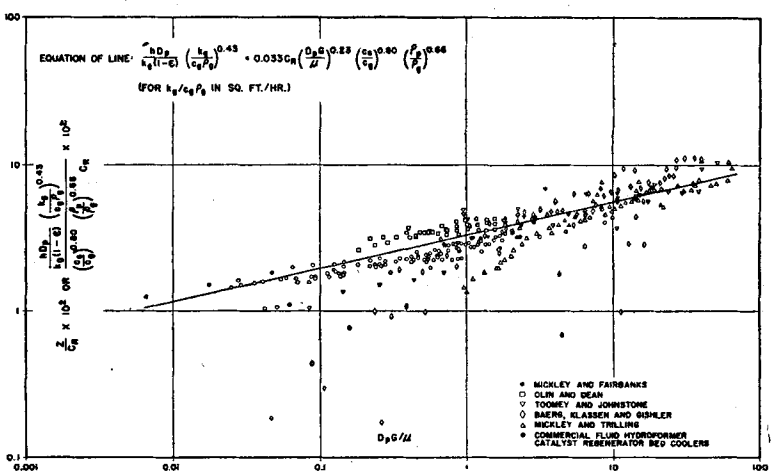

Fig. 12. The z correlation for internal heat transfer surface.

DISCUSSION OF THE CORRELATIONS

Major Deviations

Data of Mickley and Trilling, for their external surface units, show large deviations from the y correlation at low values of $1-\epsilon$, points sweeping sharply upward as vertical "tails," separated according to D_p. (See Figure 13.) These runs, which are at high velocities and which were omitted in the y correlation are believed to involve continuous vertical transport rather than true fluidized beds, with a different mechanism controlling. Even though they had disengaging sections atop their fluidization columns, some small external recycle was reported from their cyclone separators to a feed column and then to the bottoms of the fluidizing columns. In addition, inspection of their data will indicate several instances where, for a given D_p, markedly different values of ρ_b or $1-\epsilon$ were observed for runs at the same air velocity. Whereas for a fluidized bed ρ_b or $1-\epsilon$ is a unique function of gas flow rate, the behavior mentioned above is characteristic of vertical transport, where ρ_b or $1-\epsilon$ is also dependent upon the solids feed rate.

Low velocity runs of Baerg, Klassen, and Gishler deviate sharply on the z correlation, as seen in Figure 12, with separation according to particle size. The explanation is not clear. It may be due to the coordinated downward flow of particles at the wall of their internal axial heater reported by them at low velocities. Apparently at higher velocities increased side mixing causes the data to bend over and line up together within themselves and with the other data of Figure 12.

No L_H/D_T effect was observed in the external-surface data of Leva, Weintraub, and Grummer, although data of Van Heerden, et al. and of Dow and Jakob show such an effect. For this reason, the validity of the y/F correlation (Figure 8) at values of L_H/D_T less than 7 (i.e., $F > 1$) is uncertain. Somewhere below this point entrance effects, not yet rigidly defined, become prominent. The data of Dow and Jakob can be described by an expression such as developed herein; the conditions of Leva and coworkers in some way obviated an entrance effect. Of course no such qualification need be attached to the y correlation of Figure 6, which is limited to $L_H/D_T \geqq 7$.

It should be noted that only the low L_H/D_T air data of Leva et al. deviate from the y/F curve, application of the F factor causing them to plot low. Their helium data were at a high c_g, causing ϕ ($= L_Hc_g/D_Tc_s$) to be high even at low L_H/D_T and thereby giving F equal to unity and no deviation. The low L_H/D_T air data of Leva et al. were not used in drawing the lower end of Figure 8; the curve was drawn through the helium points. (This low Re_p region is determined by the data of Leva et al., which ranged down to far lower Re_p values than did other data.)

Indications of Mechanism and General Discussion

With the use of fraction solids as $Nu_p/(1-\epsilon)$, no effect was found of particle shape or particle-size distribution. Data for various shapes and D_p ranges fall in together. Of course, reliable prediction of $1-\epsilon$ values may require these factors, but use of $1-\epsilon$ as a correlating variable apparently relieves the heat transfer problem of this burden. Indeed, experimental values of $1-\epsilon$ for a particular solid can be determined quickly and easily, when required, relative to the experimental determination of heat transfer coefficients. [Fraction

TABLE 2

TERMS FOR INTERNAL HEAT TRANSFER SURFACE

$Nu_p/(1-\epsilon)$ at $Re_p = 0.35$ as a Function of Average Physical Properties

Source	Solid	Gas	ρ_p	ρ_g	c_s	c_g	k_g	$k_g/c_g\rho_g$ sq. ft./hr.	$\frac{Nu_p}{1-\epsilon}$ at $Re_p = 0.35$
20	Glass	CCl_2F_2	153	0.30	0.20	0.15	0.0061	0.136	4.2
20	Glass	Argon	153	0.11	0.20	0.125	0.011	0.800	3.95
20	Glass	Air	153	0.071	0.20	0.25	0.016	0.900	3.00
20	Glass	Ammonia	153	0.042	0.20	0.52	0.015	0.685	2.75
20	Glass	Methane	153	0.041	0.20	0.55	0.021	0.935	2.45
20	Glass	Helium	153	0.011	0.20	1.24	0.088	6.45	1.31
20	Aerocat (Cracking Cat.)	Argon	49	0.11	0.276	0.125	0.011	0.800	2.60
20	Aerocat (Cracking Cat.)	Air	49	0.071	0.276	0.25	0.016	0.900	1.91
20	Aerocat (Cracking Cat.)	Methane	49	0.041	0.276	0.55	0.021	0.935	1.39
20	Aerocat (Cracking Cat.)	Helium	49	0.011	0.276	1.24	0.088	6.45	0.92
26	Glass	Air	175	0.067	0.20	0.25	0.018	1.07	3.1
23	Sand	Air	165	0.062	0.20	0.25	0.0175	1.13	4.7

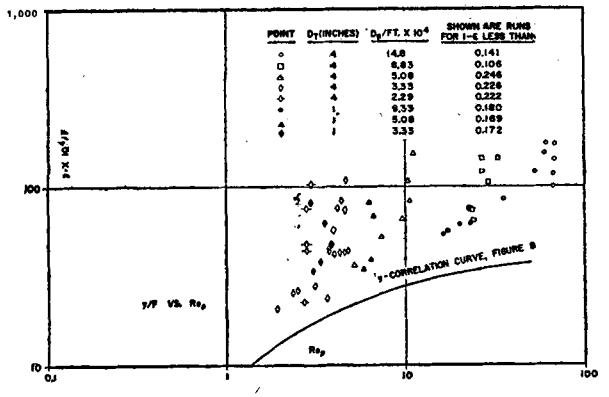

Fig. 13. Low 1 − ε data of Mickley and Trilling (external surface) showing deviations from y correlation.

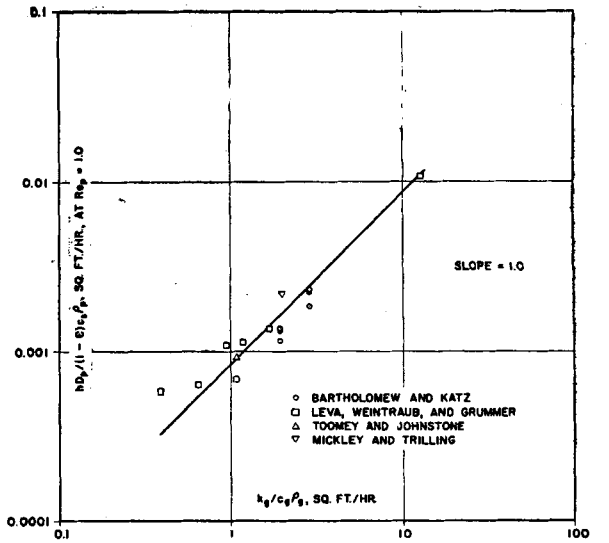

Fig. 14. Effect of gas properties on external surface heat transfer; from data at $L_H/D_T > 7$.

solids is proportional to bed density by the simple relation $\rho_b = (1 - \epsilon)\rho_p$ for gas fluidization.]

In the case of the external surface correlation, an important role for heat transport by the solid particles, as proposed by Van Heerden, Nobel, and Van Krevelen (*27*), is indicated by the dependence upon the heat-carrying capacity of the solids, $(1 - \epsilon)\ c_s\rho_p$. Writing the y correlation group as $hD_p/[(1 - \epsilon)c_s\rho_p(k_g/c_g\rho_g)]$ shows the dependence of h upon the gas thermal diffusivity in addition to dependence upon $(1 - \epsilon)\ c_s\rho_p$. The effect of gas properties as $k_g/c_g\rho_g$ is seen in Figure 14, a modification Figure 5. Here $k_g/c_g\rho_g$ is split out of the y group and plotted against $hD_p/[(1 - \epsilon)c_s\rho_p]$. The appearance of gas thermal diffusivity indicated that unsteady state conduction in the gas is important. It will be noted also that if the physical-properties terms in the y correlation group are rearranged to $k_g[(1 - \epsilon)c_s\rho_p/c_g\rho_g]$ it is as if the gas thermal conductivity in the Nusselt number were being magnified by the ratio $(1 - \epsilon)c_s\rho_p/c_g\rho_g$. The product might be interpreted as an "effective thermal conductivity" for the mobile particle suspension. This "effective thermal conductivity" should vary from a low value near the vessel wall (quiescent down flow of particles at the wall visually observed by several workers) to a very high value in the bulk of the bed [cf. high eddy conductivities reported by Gilliland (*21*)], and the group $k_g[(1 - \epsilon)c_s\rho_p/c_g\rho_g]$ may represent some mean value. With typical values (characteristic of many of the runs in the y correlation) of 0.35 for $1 - \epsilon$, 0.20 for c_s, 165 for ρ_p, 0.025 for k_g, 0.25 for c_g, and 0.050 for ρ_g, a value of 23 for the group $k_g[(1 - \epsilon)c_s\rho_p/c_g\rho_g]$ is obtained as an indication of order of magnitude of effective thermal conductivity.

As far as dependence of h upon D_p in the y correlation is concerned, it is difficult to characterize, since $1 - \epsilon$ is also dependent on D_p. Inspection of the y correlation curve (Figure 8) indicates that at low Re_p the ratio $h/(1 - \epsilon)$ or the coefficient "per unit fraction solids" increases with increasing D_p, becoming independent of D_p at intermediate Re_p values where the slope of the curve is about one, and then decreasing with decreasing D_p at high Re_p values. This behavior may explain contradictions in the literature regarding effect of D_p.

The inclusion of c_s/c_g with L_H/D_T in the external-surface L_H group ϕ is a point that requires verification. More data on physical-properties studies are needed to check this inclusion, as against a revision of the direct proportionality of $Nu_p/(1 - \epsilon)$ to $c_s\rho_p/c_g\rho_g$ to relieve the L_H/D_T group of carrying some physical properties with it. Again, Van Heerden's explanation for the L_H effect suggests possible inclusion of thermal properties with L_H/D_T.

In the case of the z correlation for internal-surface data, the complexity of the group, with separation of the ρ_p/ρ_g and c_s/c_g terms, makes analysis difficult. The importance of thermal diffusivity of the gas indicates unsteady state conduction in the gas as a major factor. Lesser variation with Reynolds number is probably due to more side mixing in the bed than at the vessel wall. Dependence of $h/(1 - \epsilon)$ upon D_p is seen to be simply $h/(1 - \epsilon) \propto D_p^{-0.77}$, showing decrease of $h/(1 - \epsilon)$ with increasing D_p in the case of internal surface. Inspection of the z correlation equation will also show ρ_g to drop out when gas mass velocity G is replaced by linear velocity as $u_g\rho_g$.

It must be remembered, of course, that the z function was established by the work of only one group (Mickley and Fairbanks) and that the other internal surface data tied in with it. There appears to be some evidence of discrepancies at low gas velocities ($G/G_{mf} < 2$).

CONCLUSION

For the first time, correlations of the data from as many as eight literature sources, plus commercial units, are reported for heat transfer to beds of fluidized solids. The correlations are

1. For external heat transfer surface, a curve (Figure 8) of the dimensionless y/F group

$$\frac{hD_p/[k_g(1 - \epsilon)(c_s\rho_p/c_g\rho_g)]}{1 + 7.5e^{-0.44(L_H/D_T)/(c_s/c_g)}}$$

vs. D_pG/μ, with five data sets included.

Table 3

Ranges of Variables Covered

	External surface y correlation	Internal surface z correlation
D_p(ft. × 10^4)	1.62–27.8	1.33–28.8
c_s	0.117–0.276	0.20–0.316
ρ_p	52–328	49–179
$1 - \epsilon$	0.050–0.564	0.055–0.603
c_g	0.235–1.24	0.125–1.24
ρ_g	0.0069–0.185	0.011–0.485
μ(centipoises)	0.0193–0.0290	0.0105–0.0382
k_g	0.0165–0.108	0.0061–0.088
D_T(ft.)	0.083–0.394	0.24–6.33
L_H(ft.)	0.142–3.33	0.33–17.5
L_B(ft.)	0.142–8.33	0.83–26.6
h	3.3–174	10.0–181

2. For internal heat transfer surface, a straight-line plot (Figure 12) of the dimensional z/C_R group

$$\frac{\dfrac{hD_p}{k_g}\left(\dfrac{k_g}{c_g\rho_g}\right)^{0.43}}{(1 - \epsilon)C_R\left(\dfrac{c_s}{c_g}\right)^{0.80}\left(\dfrac{\rho_p}{\rho_g}\right)^{0.66}}$$

vs. D_pG/μ, with six data sets included. The equation of this correlation is

$$\frac{hD_p}{k_g(1-\epsilon)}\left(\frac{k_g}{c_g\rho_g}\right)^{0.43} = 0.033C_R\left(\frac{D_pG}{\mu}\right)^{0.23}\left(\frac{c_s}{c_g}\right)^{0.80}\left(\frac{\rho_p}{\rho_g}\right)^{0.66}$$

C_R, the correlation for nonaxial tube location, is read from Figure 11.

While empirical, these correlations offer a means of predicting coefficients until better understanding of mechanism enables sounder theoretical methods to be evolved. A total of 752 runs is included, with average deviations of 22.1% for the 429 runs in the y correlation for external surface and 19.5% for the 323 runs in the z correlation for internal surface. These are considered to be fairly good, in view of the number and variety of experimental studies correlated. The inclusion of data on commercial units, in the z correlation, is particularly encouraging. Table 3 summarizes the ranges of variables covered.

Over all, the most important conclusion is that order can indeed be brought into what had previously appeared to be a chaotic situation.

ACKNOWLEDGMENT

The authors wish to thank The M. W. Kellogg Company for permission to publish this paper and W. E. Lobo and G. T. Skaperdas for their helpful guidance.

NOTATION

B = an arbitrary constant
c_g = heat capacity of the fluidizing gas, B.t.u./(lb.)(°F.)
c_s = heat capacity of solid being fluidized, B.t.u./(lb.)(°F.)
C = an arbitrary constant
C_R = correction for nonaxial-tube location, for cases of internal heat transfer surface
D_p = average particle diameter, ft.
D_T = diameter of fluidization vessel, ft.
e = base of natural logarithms
E = the group y at a Reynolds number of 1
E_0 = the group y_0 at a Reynolds number of 1
F = heated-length correction factor, $1 + 7.5e^{-0.44\phi}$, for external surface correlation
G = superficial mass velocity of gas, lb./(sec.)(sq. ft.) or lb./(hr.)(sq. ft.)
G_{mf} = minimum fluidizing mass velocity, lb./(sec.)(sq. ft.) or lb./(hr.)(sq. ft.)
h = heat transfer coefficient for transfer between bed and heating or cooling surface, B.t.u./(hr.)(sq. ft./°F.)
h_0 = constant value of external surface h at high values of heated-length group ϕ, B.t.u./(hr.)(sq. ft./°F.)
k_g = thermal conductivity of the fluidizing gas, B.t.u./(hr.)(sq. ft.)(°F./ft.)
L_B = bed height, ft.
L_H = length of heat transfer surface, ft.
L_{mf} = bed height at incipient fluidization or height of freshly settled bed, ft.
n = an arbitrary constant
Nu_p = Nusselt number, hD_p/k_g, based on average particle diameter
Pr = Prandtl number, $c_g\mu/k_g$
Re_p = Reynolds number, D_pG/μ, based on average particle diameter
R_t = radial distance of tubes from axis of shell, ft.
R_T = radius of shell or fluidizing vessel, ft.
u_g = superficial linear velocity of gas, ft./sec. or ft./hr.
y = dimensionless correlation group $hD_p/[k_g(1-\epsilon)(c_s\rho_p/c_g\rho_g)]$ for external heat transfer surface
y_0 = constant value of y at high values of heated-length group ϕ, i.e., the group y based on h_0
z = dimensional-correlation group $(hD_p/k_g)(k_g/c_g\rho_g)^{0.43}/[(1-\epsilon)(c_s/c_g)^{0.80}(\rho_p/\rho_g)^{0.66}]$ for internal heat transfer surface

Greek Letters

ϵ = fraction voids (extraparticle) in fluidized bed
$1-\epsilon$ = fraction solids in fluidized bed
ρ_b = average fluidized-bed density, lb./cu. ft.
ρ_g = density of fluidizing gas, lb./cu. ft.
ρ_p = particle density, lb./cu. ft., including internal voids for porous particles; equal to mass of particle/volume of particle
ϕ = dimensionless heated-length group $(L_H/D_T)/(c_s/c_g)$ for external heat transfer surface
μ = viscosity of the fluidizing gas, centipoises, lb./(sec.)(ft.), lb./(hr.)(ft.)

LITERATURE CITED

1. Agarwal, O. P., and J. A. Storrow, *Chem. & Ind.*, p. 321 (1951).
2. Baerg, A., J. Klassen, and P. E. Gishler, *Can. J. Research*, **28F**, 287 (1950).
3. Bartholomew, R. N., and D. L. Katz, *Chem. Eng. Progr. Symposium Ser.* No. 4, **48**, 3 (1952); also Bartholomew, R. N., Ph.D. thesis, Univ. Mich., Ann Arbor (1950).
4. Brazelton, W. T., Ph.D. thesis, Northwestern Univ., Evanston, Ill. (1951).
5. Campbell, J. R., and F. Rumford, *J. Soc. Chem. Ind.*, **69**, 373 (1950).
6. Carr, N. L., and N. R. Amundson, *Ind. Eng. Chem.*, **43**, 1856 (1951).
7. Dow, W. M., and Max Jakob, *Chem. Eng. Progr.*, **47**, 637 (1951).
8. Gamson, B. W., *Chem. Eng. Progr.*, **47**, 19 (1951).
9. Gilliland, E. R., paper presented at A.I.Ch.E. New Jersey Section Meeting (May 5, 1953).
10. Gishler, P. E., personal communication (Aug. 17, 1953).
11. Jolley, L. J., *Fuel*, **28**, 114 (1949).
12. Kettenring, K. N., E. L. Manderfield, and J. M. Smith, *Chem. Eng. Progr.*, **46**, 139 (1950).
13. Koble, R. A., J. N. Ademino, E. P. Bartkus, and T. E. Corrigan, *Chem. Eng.*, p. 174 (September, 1951).
14. Leva, Max and M. Grummer, *Chem. Eng. Progr.*, **48**, 307 (1952).
15. Leva, Max, paper presented at the General Discussion of Heat Transfer, Inst. Mech. Engrs., London (Sept. 11–13, 1951).
16. Leva, Max, M. Weintraub, and M. Grummer, *Chem. Eng. Progr.*, **45**, 563 (1949).
17. Leva, Max, communication to W. J. Danziger of The M. W. Kellogg Co.
18. Levenspiel, Octave, and J. S. Walton, *Chem. Eng. Progr. Symposium Ser.* No. 9, **50**, 1 (1954); also Octave Levenspiel, Ph.D. thesis, Oregon State College, Corvallis (1952).
19. Levenspiel, Octave and J. S. Walton, "Proc. of Heat Transfer and Fluid Mechanics Institute," p. 139, *Am. Soc. of Mech. Engrs.* (May, 1949).
20. Mickley, H. S., and D. F. Fairbanks, *A.I.Ch.E. Journal*, **1**, 374 (1955); also Fairbanks, D. F., Sc.D. thesis, Mass. Inst. Technol., Cambridge (1953).
21. Mickley, H. S., and C. A. Trilling, *Ind. Eng. Chem.*, **41**, 1135 (1949).
22. Miller, C. O., and A. K. Logwinuk, *ibid.*, **43**, 1220 (1951); also, Logwinuk, A. K., Ph.D. thesis, Case Inst. Technol., Cleveland, Ohio (1948).
23. Olin, H. L., and O. C. Dean, *The Petroleum Engineer*, p. C-23 (March, 1953); also Dean, O. C., Ph.D. thesis, Univ. Iowa, Ames (1952).
24. Pritzlaff, A. H., Jr., Ph.D. thesis, Northwestern Univ., Evanston, Ill. (1951).
25. Simon, R. H., Ph.D. thesis, Oregon State College, Corvallis (1948).
26. Toomey, R. D., and H. F. Johnstone, *Chem. Eng. Progr. Symposium Ser.* No. 5, **49**, 51 (1953); also Toomey, R. D., Ph.D. thesis, Univ. of Illinois, Urbana (1950).
27. Van Heerden, C., A. P. P. Nobel, and D. W. Van Krevelen, *Ind. Eng. Chem.*, **45**, 1237 (1953).
28. Van Heerden, C., *J. Appl. Chem.*, **2**, Supplementary Issue No. 1, S-7 (1952).
29. ———, A. P. P. Nobel, and D. W. Van Krevelen, paper presented at the General Discussion of Heat Transfer, Inst. Mech. Engrs., London (Sept. 11–13, 1951).
30. ———, *Chem. Eng. Sci.*, **1**, 51 (1951).
31. Vreedenberg, H. A., *J. Appl. Chem.*, **2**, Supplementary Issue No. 1, S-26 (1952).
32. Vreedenberg, H. A., paper presented at the General Discussion of Heat Transfer, Inst. Mech. Engrs., London (Sept. 11–13, 1951).
33. Walton, J. S., R. L. Olson, and Octave Levenspiel, *Ind. Eng. Chem.*, **44**, 1474 (1952).
34. Wamsley, W. E., and L. N. Johanson, *Chem. Eng. Progr.*, **50**, 347 (1954).
35. Wen, C. Y., and Max Leva, *A.I.Ch.E. Journal*, **2**, 482 (1956).

Manuscript submitted May, 1957; revision received September 3, 1957; paper accepted September 9, 1957.